

## MULTIWAVELENGTH OBSERVATIONS OF 3C 454.3. II. THE *AGILE* 2007 DECEMBER CAMPAIGN

I. DONNARUMMA<sup>1,25</sup>, G. PUCELLA<sup>1</sup>, V. VITTORINI<sup>1</sup>, F. D’AMMANDO<sup>1,2</sup>, S. VERCELLONE<sup>3</sup>, C. M. RAITERI<sup>4</sup>, M. VILLATA<sup>4</sup>, M. PERRI<sup>5</sup>, W. P. CHEN<sup>6</sup>, R. L. SMART<sup>4</sup>, J. KATAOKA<sup>7</sup>, N. KAWAI<sup>7</sup>, Y. MORI<sup>7</sup>, G. TOSTI<sup>8</sup>, D. IMPIOMBATO<sup>8</sup>, T. TAKAHASHI<sup>9</sup>, R. SATO<sup>9</sup>, M. TAVANI<sup>1,2</sup>, A. BULGARELLI<sup>10</sup>, A. W. CHEN<sup>11</sup>, A. GIULIANI<sup>11</sup>, F. LONGO<sup>12</sup>, L. PACCIANI<sup>1</sup>, A. ARGAN<sup>1</sup>, G. BARBIELLINI<sup>12</sup>, F. BOFFELLI<sup>13</sup>, P. CARAVEO<sup>11</sup>, P. W. CATTANEO<sup>13</sup>, V. COCCO<sup>1</sup>, T. CONTESSI<sup>11</sup>, E. COSTA<sup>1</sup>, E. DEL MONTE<sup>1</sup>, G. DE PARIS<sup>1</sup>, G. DI COCCO<sup>10</sup>, Y. EVANGELISTA<sup>1</sup>, M. FEROCI<sup>1</sup>, A. FERRARI<sup>14,15</sup>, M. FIORINI<sup>11</sup>, T. FROYSLAND<sup>14</sup>, M. FRUTTI<sup>1</sup>, F. FUSCHINO<sup>10</sup>, M. GALLI<sup>16</sup>, F. GIANOTTI<sup>10</sup>, C. LABANTI<sup>10</sup>, I. LAPSHOV<sup>1</sup>, F. LAZZAROTTO<sup>1</sup>, P. LIPARI<sup>17</sup>, M. MARISALDI<sup>10</sup>, M. MASTROPIETRO<sup>18</sup>, S. MEREGHETTI<sup>11</sup>, E. MORELLI<sup>10</sup>, E. MORETTI<sup>12</sup>, A. MORSELLI<sup>19</sup>, A. PELLIZZONI<sup>20</sup>, F. PEROTTI<sup>11</sup>, G. PIANO<sup>1,2</sup>, P. PICOZZA<sup>19</sup>, M. PILIA<sup>20,21</sup>, G. PORROVECCHIO<sup>1</sup>, M. PREST<sup>21</sup>, M. RAPISARDA<sup>22</sup>, A. RAPPOLDI<sup>13</sup>, A. RUBINI<sup>1</sup>, S. SABATINI<sup>1</sup>, E. SCALISE<sup>1</sup>, P. SOFFITTA<sup>1</sup>, E. STRIANI<sup>1,2</sup>, M. TRIFOGLIO<sup>10</sup>, A. TROIS<sup>1</sup>, E. VALLAZZA<sup>12</sup>, A. ZAMBRA<sup>11</sup>, D. ZANELLO<sup>17</sup>, C. PITTORI<sup>5</sup>, P. SANTOLAMAZZA<sup>5</sup>, F. VERRECCHIA<sup>5</sup>, P. GIOMMI<sup>5</sup>, L. A. ANTONELLI<sup>23</sup>, S. COLAFRANCESCO<sup>5</sup>, AND L. SALOTTI<sup>24</sup>

<sup>1</sup> INAF/IASF–Rome, Via del Fosso del Cavaliere 100, I-00133 Rome, Italy; [immacolata.donnarumma@iasf-roma.inaf.it](mailto:immacolata.donnarumma@iasf-roma.inaf.it)

<sup>2</sup> Dip. di Fisica, Univ. “Tor Vergata,” Via della Ricerca Scientifica 1, I-00133 Rome, Italy

<sup>3</sup> INAF/IASF Palermo Via Ugo La Malfa 153, 90146 Palermo, Italy

<sup>4</sup> INAF/OATo, Via Osservatorio 20, I-10025 Pino Torinese, Italy

<sup>5</sup> ASI–ASDC, Via G. Galilei, I-00044 Frascati (Rome), Italy

<sup>6</sup> Institute of Astronomy, National Central University, Taiwan

<sup>7</sup> Department of Physics, Tokyo Institute of Technology, Tokyo, Japan

<sup>8</sup> Dip. di Fisica, Univ. di Perugia, Via Pascoli, I-06123 Perugia, Italy

<sup>9</sup> ISAS/JAXA, 3-1-1 Yoshinodai, Sagamihara, Kanagawa 229-8510, Japan

<sup>10</sup> INAF/IASF–Bologna, Via Gobetti 101, I-40129 Bologna, Italy

<sup>11</sup> INAF/IASF–Milano, Via E. Bassini 15, I-20133 Milan, Italy

<sup>12</sup> Dip. di Fisica and INFN Trieste, Via Valerio 2, I-34127 Trieste, Italy

<sup>13</sup> INFN–Pavia, Via Bassi 6, I-27100 Pavia, Italy

<sup>14</sup> CIFS–Torino, Viale Settimio Severo 63, I-10133 Turin, Italy

<sup>15</sup> Dip. di Fisica Generale dell’Università, Via Pietro Giuria 1, I-10125 Turin, Italy

<sup>16</sup> ENEA, Via Martiri di Monte Sole 4, I-40129 Bologna, Italy

<sup>17</sup> INFN–Rome “La Sapienza,” Piazzale A. Moro 2, I-00185 Rome, Italy

<sup>18</sup> Consiglio Nazionale delle Ricerche, Istituto Metodologie Inorganiche e dei Plasmi, Area Ricerca Montelibretti (Rome), Italy

<sup>19</sup> INFN–Rome “Tor Vergata,” Via della Ricerca Scientifica 1, I-00133 Rome, Italy

<sup>20</sup> INAF–Osservatorio Astronomico di Cagliari, localit Poggio dei Pini, Strada 54, I-09012 Capoterra, Italy

<sup>21</sup> Dip. di Fisica, Univ. dell’Insubria, Via Valleggio 11, I-22100 Como, Italy

<sup>22</sup> ENEA–Rome, Via E. Fermi 45, I-00044 Frascati (Rome), Italy

<sup>23</sup> Osservatorio Astronomico di Roma, Monte Porzio Catone (Rome), Italy

<sup>24</sup> ASI, Viale Liegi 26, I-00198 Rome, Italy

Received 2009 June 23; accepted 2009 October 29; published 2009 December 2

### ABSTRACT

We report on the second *Astrorivelatore Gamma a Immagini Leggero (AGILE)* multiwavelength campaign of the blazar 3C 454.3 during the first half of 2007 December. This campaign involved *AGILE*, *Spitzer*, *Swift*, *Suzaku*, the Whole Earth Blazar Telescope (WEBT) consortium, the Rapid Eye Mount (REM), and the Multicolor Imaging Telescopes for Survey and Monstrous Explosions (MITSuME) telescopes, offering a broadband coverage that allowed for a simultaneous sampling of the synchrotron and inverse Compton (IC) emissions. The two-week *AGILE* monitoring was accompanied by radio to optical monitoring by WEBT and REM, and by sparse observations in mid-infrared and soft/hard X-ray energy bands performed by means of Target of Opportunity observations by *Spitzer*, *Swift*, and *Suzaku*, respectively. The source was detected with an average flux of  $\sim 250 \times 10^{-8}$  photons  $\text{cm}^{-2} \text{s}^{-1}$  above 100 MeV, typical of its flaring states. The simultaneous optical and  $\gamma$ -ray monitoring allowed us to study the time lag associated with the variability in the two energy bands, resulting in a possible  $\lesssim$ one-day delay of the  $\gamma$ -ray emission with respect to the optical one. From the simultaneous optical and  $\gamma$ -ray fast flare detected on December 12, we can constrain the delay between the  $\gamma$ -ray and optical emissions within 12 hr. Moreover, we obtain three spectral energy distributions (SEDs) with simultaneous data for 2007 December 5, 13, and 15, characterized by the widest multifrequency coverage. We found that a model with an external Compton on seed photons by a standard disk and reprocessed by the broad-line regions does not describe in a satisfactory way the SEDs of 2007 December 5, 13, and 15. An additional contribution, possibly from the hot corona with  $T = 10^6$  K surrounding the jet, is required to account simultaneously for the softness of the synchrotron and the hardness of the IC emissions during those epochs.

**Key words:** galaxies: active – galaxies: individual (3C 454.3) – galaxies: jets – gamma rays: observations – quasars: general – radiation mechanisms: non-thermal

**Online-only material:** color figures

## 1. INTRODUCTION

3C 454.3 is a flat spectrum radio quasar at redshift  $z = 0.859$ . It is one of the brightest extragalactic radio sources with superluminal motion hosting a radio and an X-ray jet. It has been observed in almost all the electromagnetic spectrum from radio up to  $\gamma$ -ray energies; the spectral energy distribution (SED) has the typical double-humped shape of blazars, the first peak occurring at mid-far-infrared frequencies and the second one at MeV–GeV energies (see Ghisellini et al. 1998).

The first peak is commonly interpreted as synchrotron radiation from high-energy electrons in a relativistic jet, while the second component is due to electrons scattering on soft seed photons. In the context of a simple, homogeneous scenario, the emission at the synchrotron and inverse Compton (IC) peaks is produced by the same electron population that can self-scatter the same synchrotron photons (synchrotron self-Compton, SSC). Alternatively, the jet-electrons producing the synchrotron flux can Compton-scatter seed photons produced outside of the jet (external Compton, EC).

3C 454.3 is a highly variable blazar source. In spring 2005, 3C 454.3 experienced a strong outburst in the optical band reaching its historical maximum with  $R = 12.0$  mag (Villata et al. 2006). The exceptional event triggered observations at higher energies from *Chandra* (Villata et al. 2006), *Swift* (Giommi et al. 2006), and the *International Gamma-Ray Astrophysics Laboratory* (*INTEGRAL*; Pian et al. 2006). The available data allowed the building of the spectrum of the source up to 200 keV. In particular, *INTEGRAL* detected (2005 May 15–18) the source from 3 up to 200 keV in a very bright state ( $\sim 5 \times 10^{-10}$  erg cm $^{-2}$  s $^{-1}$ ), being almost a factor of 2–3 higher than the previously observed fluxes (see Tavecchio et al. 2002). Pian et al. (2006) compared the SED in 2000 with that obtained during the 2005 outburst. They were able to describe both observed SEDs with minimal changes in the jet power, assuming that the dissipation region (where most of the radiation is produced) was inside the broad-line region (BLR) in 2000 and outside of it in 2005. On the other hand, Sikora et al. (2008) argued that X-rays and  $\gamma$ -rays could be produced via IC scattering of near- and mid-IR photons emitted by the hot dust: a very moderate energy density of the dust radiation is sufficient to provide the dominance of the EC luminosities over the SSC ones.

In 2007 July, the source woke up again in the optical band, reaching a maximum at  $R = 12.6$  mag (Raiteri et al. 2008b). Such an increase in the optical activity triggered observations with *Swift* and the *Astrorivelatore Gamma a Immagini Leggero* (*AGILE*). Although still in its Science Verification phase, *AGILE* repointed at 3C 454.3 and detected it in high  $\gamma$ -ray activity. The average  $\gamma$ -ray flux detected by *AGILE* was the highest  $\gamma$ -ray flux ever detected from this blazar,  $(280 \pm 40) \times 10^{-8}$  photons cm $^{-2}$  s $^{-1}$  (see Figure 3, lower panel, in Vercellone et al. 2008).

Ghisellini et al. (2007) reproduced the three source states in 2000, 2005, and 2007 with the model proposed in Katarzyński & Ghisellini (2007). The model assumes that the relative importance of synchrotron and SSC luminosity with respect to the EC one is controlled by the value of the bulk Lorentz factor  $\Gamma$ , which is associated with the compactness of the source.

Villata et al. (2007) and Raiteri et al. (2008b) suggested an alternative interpretation involving changes of the viewing angle of the different emitting regions of the jet.

In both cases, a strong degeneracy of parameters exists in both SSC and EC models especially when the  $\gamma$ -ray data are missing. This is the case of both SEDs in 2000 and 2005 in which historical EGRET data were used to constrain the models.

3C 454.3 exhibited outbursts several times between 2007 and 2008 (see Vercellone et al. 2008; Tosti et al. 2008; Raiteri et al. 2008a, 2008b; Vercellone et al. 2009), posing stringent constraints on its  $\gamma$ -ray duty cycle.

This strengthened the need for simultaneous observations in different energy bands. In the case of 3C 454.3 (and other MeV blazars), it is clear that the dominant contribution in the SED comes from IR–optical bands, where the synchrotron peak lies, and from both X-rays and  $\gamma$ -ray energy range, where the IC emission lies.

In this paper, we present and discuss the result of a multiwavelength campaign on 3C 454.3 during a period of intense  $\gamma$ -ray activity that occurred between 2007 December 1 and 16. In Section 2, we present the multiwavelength campaign, and in Sections 3–7 we present the *AGILE*, *Suzaku*, *Swift*, *Spitzer*, Rapid Eye Mount (REM), Whole Earth Blazar Telescope (WEBT), and Multicolor Imaging Telescopes for Survey and Monstrous Explosions (MITSuME) observations and data analysis; in Section 8, we analyze the  $\gamma$ –optical correlation and present broadband SEDs built with simultaneous data, discussing in details how they are modeled in the framework of SSC and EC scenarios. Throughout this paper, the photon indices are parameterized as  $N(E) \propto E^{-\Gamma}$  (photons cm $^{-2}$  s $^{-1}$  keV $^{-1}$  or MeV $^{-1}$ ). The uncertainties are given at  $1\sigma$  level, unless otherwise stated.

## 2. THE MULTIWAVELENGTH CAMPAIGN

During the period of intense  $\gamma$ -ray activity showed in 2007 November (Vercellone et al. 2009), *AGILE* continued the pointing toward 3C 454.3 for the first half of 2007 December. The persistent high  $\gamma$ -ray activity of the source stimulated us to activate a new multiwavelength campaign.

*AGILE* data were collected between 2007 December 1 and 2007 December 16. *Suzaku* data were collected during a dedicated Target of Opportunity (ToO) performed on December 5, whereas the *Spitzer* data were collected on December 13 and 15, thanks to a granted Director’s Discretionary Time (DDT) observation.

During these two days, a ToO with *Swift* data was activated for a total exposure of 9 ks.

During the whole *AGILE* observation, the source was monitored in radio-to-optical bands by WEBT (see Raiteri et al. 2008a). In addition, observations in the NIR and optical energy bands by REM occurred between December 1 and 8. Moreover, optical data from the MITSuME telescope are available on this source until December 6. In the following sections, we report on the details of the observations and the data analysis for each instrument.

## 3. AGILE OBSERVATION

*AGILE* (Tavani et al. 2008, 2009) is a mission of the Italian Space Agency (ASI) for the exploration of  $\gamma$ -ray sky, operating in a low Earth orbit since 2007 April 23. The *AGILE* scientific instrument (Prest et al. 2003; Perotti et al. 2006; Labanti et al. 2009) is very compact and combines four active detectors yielding simultaneous coverage in  $\gamma$ -rays, 30 MeV–30 GeV, and in hard X-ray energy band, 18–60 keV (Feroci et al. 2007).

<sup>25</sup> *AGILE* Team corresponding author

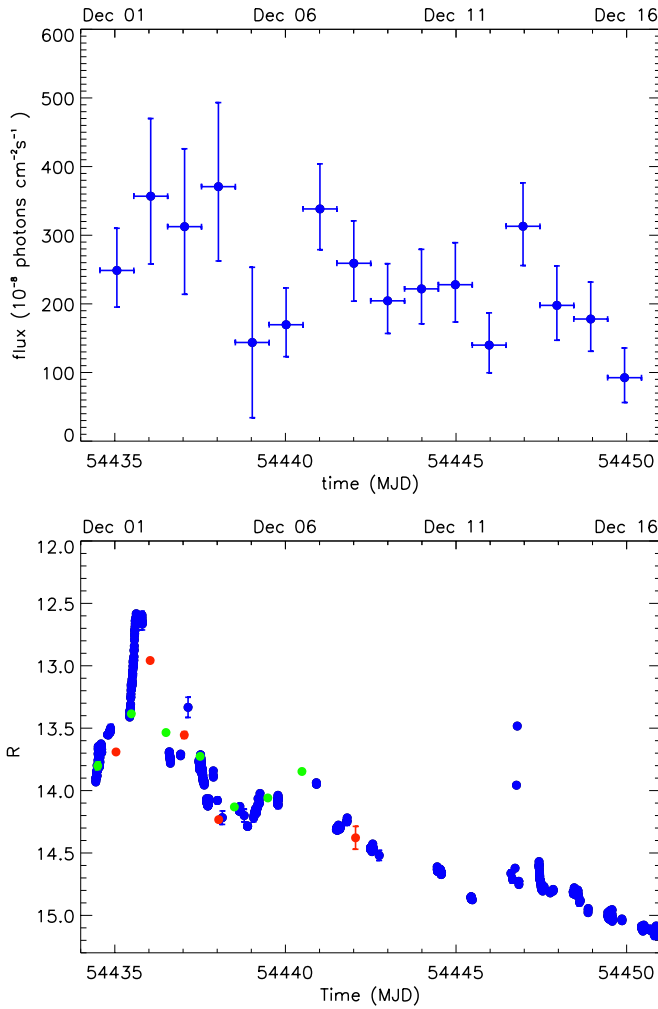


**Figure 1.** Top panel: *AGILE*-GRID  $\gamma$ -ray light curve of 3C 454.3 at one-day resolution for  $E > 100$  MeV in units of  $10^{-8}$  photons  $\text{cm}^{-2} \text{s}^{-1}$  during the period from 2007 November 30 to December 16; bottom panel:  $R$ -band light curve obtained by WEBT (blue circles), REM (red circles), and MITSuME (green circles) between November 30 and December 16.

The *AGILE* observations of 3C 454.3 were performed between 2007 December 1 and 16, for a two-week total pointing duration. In the first period, between December 1 and 5, the source was located  $\sim 45^\circ$  off the *AGILE* pointing direction. In the second period, between December 5 and 16, after a satellite re-pointing, the source was located at  $\sim 30^\circ$  off-axis (variable by  $\sim 1^\circ$  per day due to the pointing drift) to increase the significance of the detection.

*AGILE*-Gamma Rays Imaging Detector (*AGILE*-GRID) data were analyzed using the Standard Analysis Pipeline. Counts, exposure, and Galactic background maps were created with a bin size of  $0.3 \times 0.3$  for photons with energy greater than 100 MeV. To reduce the particle background contamination we selected only events flagged as confirmed  $\gamma$ -ray events, and all events collected during the South Atlantic Anomaly were rejected. We also reduced the  $\gamma$ -ray Earth albedo contamination by excluding regions within  $\sim 10^\circ$  from the Earth limb.

The two-week data have been divided into two sets taking into account the two different pointings during which the source shifted from  $\sim 45^\circ$  to  $\sim 30^\circ$  off-axis: the first set between UTC 2007 December 1 13:21 and UTC 2007 December 5 12:34; and the second set between UTC 2007 December 5 12:35 and 2007

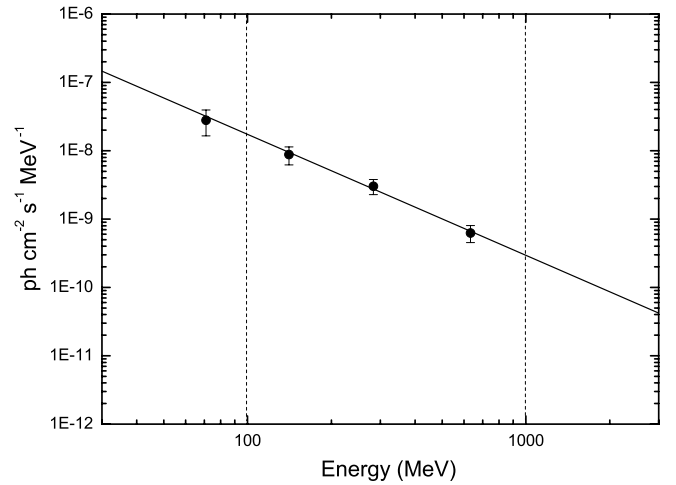


**Figure 2.** Gamma-ray photon spectrum of 3C 454.3 during the observation period 2007 December 5–16. Only the energy bins above 100 MeV were taken into account in the spectral fitting. The solid line corresponds to a power-law function with a photon index of  $\Gamma = 1.78 \pm 0.14$ .

December 16 10:27 (in Figure 1, top panel, we also report the  $\gamma$ -ray flux of one day before). The first set required a more detailed analysis due to uncertainty on calibration for large off-axis angles in the field of view (FoV).

We ran the *AGILE* maximum likelihood procedure on each data set in order to obtain the average flux as well as the daily values in the  $\gamma$ -ray band, according to Mattox et al. (1996). The average fluxes obtained by integrating separately the two data sets are  $(280 \pm 50) \times 10^{-8}$  photons  $\text{cm}^{-2} \text{s}^{-1}$  ( $\sqrt{TS} \sim 8$ ) and  $(210 \pm 16) \times 10^{-8}$  photons  $\text{cm}^{-2} \text{s}^{-1}$  ( $\sqrt{TS} \sim 20$ ) for the first and second periods, respectively. The source was always detected on the two-week period with a daily integration time. The one-day binned light curve shows three enhancements of the emission around December 4, December 7, and December 13 (see Figure 1, top panel). In particular, the last two enhancements are characterized by a sharp increase of the emission followed by a slow recovery. We accumulated the spectrum over the second set of data in which the source was positioned within  $30^\circ$  in the *AGILE*-GRID FoV, where the most significant energy spectrum can be extracted due to the higher statistical quality. The spectral fit was performed by using only data between 100 MeV and 1 GeV (which are better calibrated) although in Figure 2, we report also the energy bin below 100 MeV. It resulted in a power law with a photon index of  $\Gamma = 1.78 \pm 0.14$ . We note that the current *AGILE* response is calibrated up to 1 GeV, and that the energy flux above 1 GeV is underestimated by a factor of 2–3. This prevented us from discussing any possible spectral break above 1 GeV as found by *Fermi* (Abdo et al. 2009). However, we note that the *AGILE* spectrum seems to be harder than the one inferred by *Fermi* below  $\sim 3$  GeV. The different energy range and the non-simultaneity of the data could explain the difference between the photon indices.

Super*AGILE* did not detect the source during the two-week *AGILE* pointing. A deep  $3\sigma$  upper limit of  $\sim 10$  mcrab was derived integrating all the data in which the source was within  $30^\circ$  in the FoV (net source exposure of 360 ks).

#### 4. *SUZAKU* OBSERVATION

Following the *AGILE* detection of the flaring state, 3C 454.3 was observed with *Suzaku* (Mitsuda et al. 2007) on 2007 December 5 as a ToO, with a total duration of 40 ks. *Suzaku*

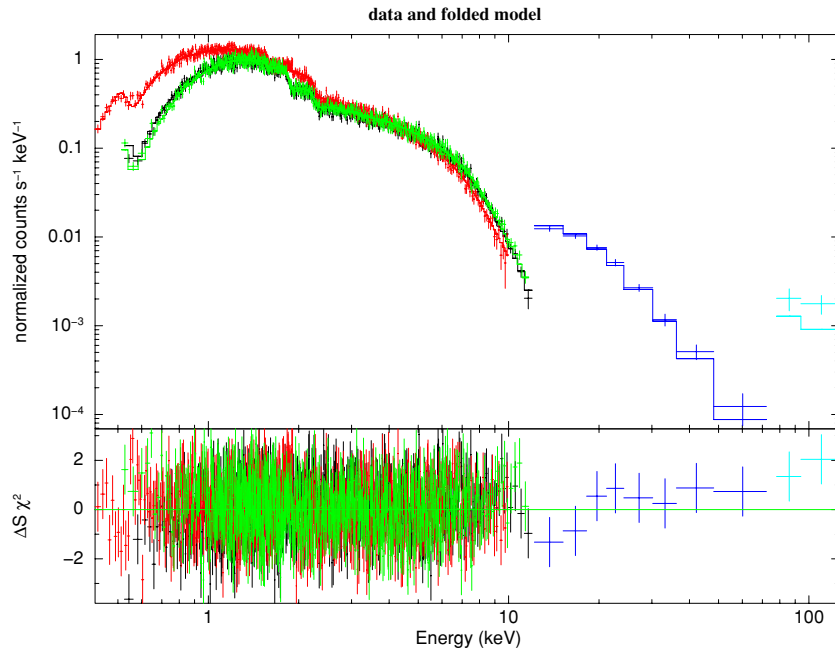


**Figure 3.** *Suzaku* broadband spectrum (XIS, PIN, GSO) of 3C 454.3 for the observation carried out in 2007 December. In the folded model, a single power law over the whole energy range is assumed; see the text for details. In the online journal, black, red, and green colors refer to XIS0, XIS1, and XIS3, respectively; blue points to PIN; cyan points to GSO.

(A color version of this figure is available in the online journal.)

carries four sets of X-ray telescopes (Serlemitsos et al. 2007), each one equipped with a focal-plane X-ray CCD camera (X-ray Imaging Spectrometer, XIS; Koyama et al. 2007) that is sensitive in the energy range of 0.3–12 keV, together with a non-imaging hard X-ray detector (HXD; Takahashi et al. 2007; Kokubun et al. 2007), which covers the 10–600 keV energy band with Si PIN photodiodes and GSO scintillation detectors. 3C 454.3 was focused on the nominal center position of the XIS detectors.

For the XIS, we analyzed the screened data, reduced via *Suzaku* software version 2.1. The reduction followed the prescriptions described in “The *Suzaku* Data Reduction Guide” provided by the *Suzaku* guest observer facility at NASA/GSFC.<sup>26</sup> The screening was based on the following criteria: (1) only ASCA-grade 0, 2, 3, 4, and 6 events are accumulated, while hot and flickering pixels were removed from the XIS image using the CLEANIS script, (2) the time interval after the passage through the South Atlantic Anomaly (T\_SAA\_HXD) is greater than 500 s, (3) the object is at least 5° and 20° above the rim of the Earth (ELV) during night and day, respectively. In addition, we also selected the data with a cutoff rigidity (COR) larger than 6 GV. After this screening, the net exposure for good time intervals (GTIs) is 35.1 ks. The XIS events were extracted from a circular region with a radius of 4'3 centred on the source peak, whereas the background was accumulated in an annulus with inner and outer radii of 5'0 and 7'0 pixels, respectively. The response (RMF) and auxiliary (ARF) files are produced using the analysis tools XISRMFGEN and XISSIMARFGEN, which are included in the software package HEASoft version 6.4.1.

The HXD/PIN event data (version 2.1) are processed with basically the same screening criteria as those for the XIS, except that  $\text{ELV} \geq 5^\circ$  through night and day, and  $\text{COR} \geq 8$  GV.

The HXD/PIN instrumental background spectra were generated from a time-dependent model provided by the HXD instrument team for each observation (see Kokubun et al. 2007). Both the source and background spectra were made with identical GTIs and the exposure was corrected for a detector dead time of 6.9%. We used the response files version AE\_HXD\_PINXINOME\_20070914.RSP, provided by the HXD instrumental team. Similarly, the HXD/GSO event data (ver. 2.1) were processed with a standard analysis technique described in the cited “The *Suzaku* Data Reduction Guide.” Despite the relatively high instrumental background of the HXD/GSO, the source was marginally detected at  $5.5\sigma$  level between 80 and 120 keV. We used the response files version AE\_HXD\_GSOXINOM\_20080129.RSP. Spectral analysis was performed using the Xspec fitting package 12.3.1. and we fitted both the soft and hard X-ray spectra with a power law with Galactic absorption free to vary. The XIS spectra are well fitted with a power law with  $\Gamma = 1.63$  absorbed with  $N_{\text{H}} = 1.1 \times 10^{21} \text{ cm}^{-2}$ , which infers the absorbed fluxes of  $4.51^{+0.07}_{-0.03} \times 10^{-11} \text{ erg cm}^{-2} \text{ s}^{-1}$  and  $3.20^{+0.04}_{-0.01} \times 10^{-11} \text{ erg cm}^{-2} \text{ s}^{-1}$  in the energy bands 0.3–10 keV and 2–10 keV, respectively. The hard X-ray spectrum determined by HXD/PIN and GSO seems to be a bit flatter than those determined by the XIS only below 10 keV, as it is shown in the residuals reported in Figure 3 (where a model with a single power law is assumed). We found that it is better fitted by a power-law photon index of  $\Gamma = 1.35 \pm 0.14$ , which gives  $F_{10-100 \text{ keV}} = 1.37^{+0.1}_{-0.08} \times 10^{-10} \text{ erg cm}^{-2} \text{ s}^{-1}$ . The uncertainties reported above are at 90% confidence level.

## 5. SWIFT OBSERVATION

During our campaign *Swift* (Gehrels et al. 2004) performed two ToO observations of 3C 454.3: the first on 2007 December 13, the second on 2007 December 15. Both observations were performed using all onboard experiments: the X-ray Telescope

<sup>26</sup> <http://suzaku.gsfc.nasa.gov/docs/suzaku/analysis/abc>. See also seven steps to the *Suzaku* data analysis at <http://www.astro.isas.jaxa.jp/suzaku/analysis>.



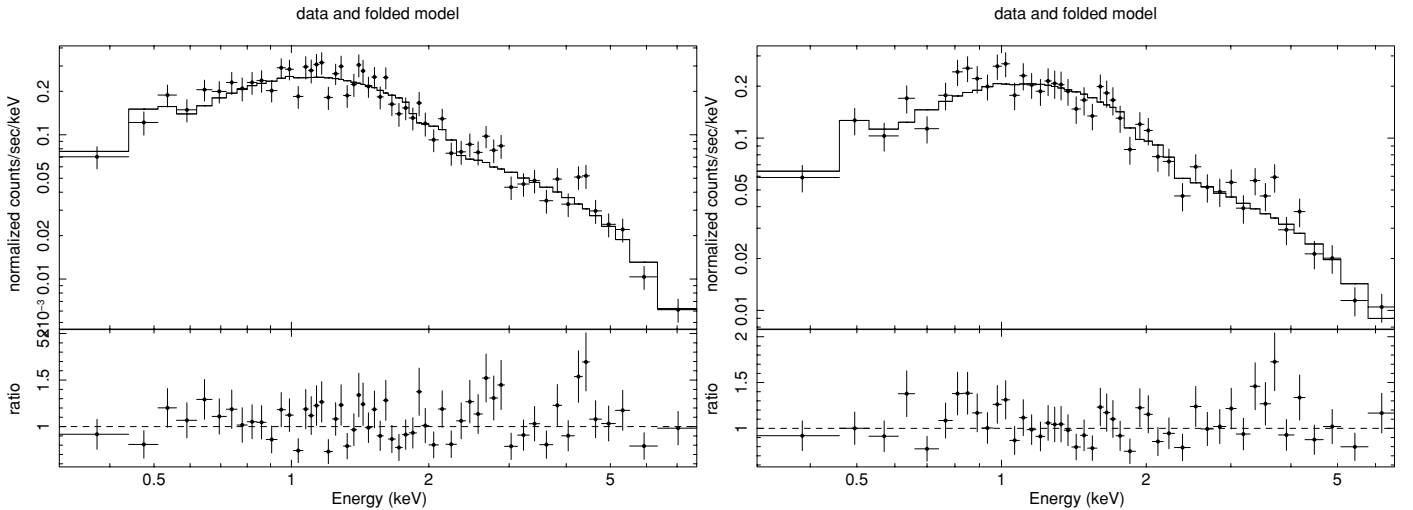


**Figure 4.** *Swift* data and the folded model of 3C 454.3 for the observation carried out in 2007 December 13 (left panel) and 15 (right panel).

**Table 1**  
Results of XRT Observations of 3C 454.3

Observation Date	$N_{\text{H}}$ ( $10^{22} \text{ cm}^{-2}$ )	Flux 0.3–10 keV ( $\text{erg cm}^{-2} \text{ s}^{-1}$ )	Flux 2–10 keV ( $\text{erg cm}^{-2} \text{ s}^{-1}$ )	Spectral Slope $\Gamma$	$\chi^2/\text{d.o.f.}$
2007 Dec 13	$0.13 \pm 0.03$	$(4.38 \pm 0.25) \times 10^{-11}$	$(3.04 \pm 0.24) \times 10^{-11}$	$1.74 \pm 0.10$	1.28/54
2007 Dec 15	$0.14 \pm 0.03$	$(3.60 \pm 0.22) \times 10^{-11}$	$(2.49 \pm 0.22) \times 10^{-11}$	$1.76 \pm 0.12$	1.14/44

**Note.** The power-law model with  $N_{\text{H}}$  free to vary.

(XRT; Burrows et al. 2005; 0.2–10 keV), the UV and Optical Telescope (UVOT; Roming et al. 2005; 170–600 nm), and the Burst Alert Telescope (BAT; Barthelmy et al. 2005; 15–150 keV). The hard X-ray flux of this source is below the sensitivity of the BAT instrument for short exposure and therefore the data from this instruments will not be used. We refer to Raiteri et al. (2008a) for a detailed description of data reduction and analysis of the UVOT data.

XRT observations were carried out using the instrument in photon counting (PC) readout mode (see Burrows et al. 2005 and Hill et al. 2004 for details of the XRT observing modes). The XRT data were processed with the XRTDAS software package (ver. 2.2.2) developed at the ASI Science Data Center (ASDC) and distributed by HEASARC within the HEASoft package (ver. 6.4). Event files were calibrated and cleaned with standard filtering criteria with the *xrtpipeline* task using the latest calibration files available in the *Swift* CALDB distributed by HEASARC. Both observations showed an average count rate of  $>0.5 \text{ counts s}^{-1}$  and therefore pile-up correction was required. We extracted the source events from an annulus extraction region with inner and outer radii of 3 and 30 pixels, respectively. To account for the background, we also extracted events within a circular region centred on a region free from background sources and with a radius of 80 pixels. The ancillary response files were generated with the task *xrtmkarf*. We used the latest spectral redistribution matrices (RMF, ver. 011) in the Calibration Database maintained by HEASARC. The adopted energy range for spectral fitting is 0.3–10 keV, and all data are rebinned with a minimum of 20 counts per energy bin to use the  $\chi^2$  statistics. *Swift*/XRT uncertainties are given at 90% confidence level for one interesting parameter, unless otherwise stated.

Spectral analysis was performed using the Xspec fitting package 12.3.1 and we fitted the spectra with a power-law model with galactic absorption left free to vary. In Table 1, we summarize the best-fit parameters and the derived absorbed fluxes in the energy ranges 0.3–10 keV and 2–10 keV. We note that the best-fit  $N_{\text{H}}$  values in Table 1 are in agreement with the value  $1.34 \times 10^{21} \text{ cm}^{-2}$  derived by Villata et al. (2006) when analyzing *Chandra* observations in 2005 May, and adopted by Raiteri et al. (2007, 2008b) when fitting the X-ray spectra acquired by *XMM-Newton* in 2006–2007. In Figure 4, we show the data and the folded models for these observations.

## 6. OPTICAL MONITORING

### 6.1. WEBT Observation

The WEBT (<http://www.oato.inaf.it/blazars/webt/>) is an international collaboration including tens of optical, near-IR, and radio astronomers devoted to blazar studies. An extensive monitoring effort on 3C 454.3 was carried out by the WEBT from 2005 to 2008, to follow the large 2005 outburst and post-outburst phases (Villata et al. 2006, 2007; Raiteri et al. 2007), and the new flaring phase started in mid 2007 (Raiteri et al. 2008a, 2008b). A detailed presentation and discussion of the radio, millimetric, optical, and *SWIFT*-UVOT data collected in 2007 December can be found in Raiteri et al. (2008a). Here we adopt their data analysis in the context of our multifrequency study.

### 6.2. REM Observation

The photometric optical observations were carried out with the REM (Zerbi et al. 2004), a robotic telescope located at the ESO Cerro La Silla observatory (Chile). The REM telescope has

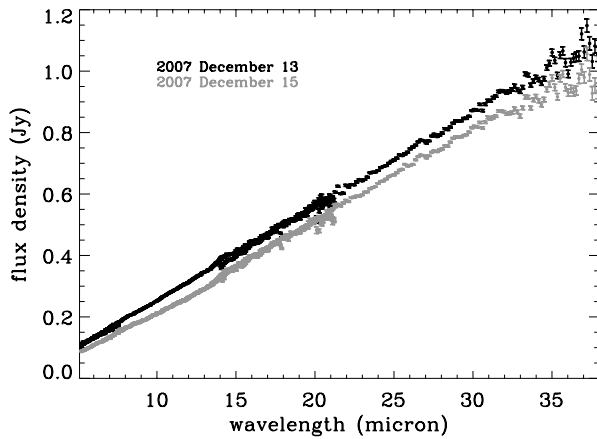


**Figure 5.** *Spitzer* spectra of 3C 454.3 for the observation carried out in 2007 December 13 (black points) and 15 (gray points).

a Ritchey–Chretien configuration with a 60 cm  $f/2.2$  primary and an overall  $f/8$  focal ratio in a fast moving alt-azimuth mount providing two stable Nasmyth focal stations. Two cameras are simultaneously used at the focus of the telescope, by means of a dichroic filter, REMIR for the NIR (Conconi et al. 2004) and ROSS for the optical (Tosti et al. 2004), in order to obtain nearly simultaneous data.

The telescope REM has observed 3C 454.3 between 2007 December 1 and December 8, overlapping with the *AGILE* observation period. The light curve produced by REM in the  $R$  band is shown in Figure 1 (bottom panel, red points).

### 6.3. *MiSuME* Observation

A contribution of the optical follow-up observations was given also by *MiSuME*, composed of three robotic telescopes (of 50 cm diameter each) located at the Institute of Cosmic-ray Research (ICRR) Akeno Observatory, Yamanashi, Japan and the Okayama Astrophysical Observatory (OAO). Each *MiSuME* telescope has a tricolor camera, which allows us to take simultaneous images in  $g'$ ,  $R_c$ , and  $I_c$  bands. The camera employs three Alta U-6 cameras (Apogee Instruments Inc.) and KAF-1001E CCD (Kodak) with  $1024 \times 1024$  pixels. The pixel size is  $24 \mu\text{m} \times 24 \mu\text{m}$ , or  $1''.6 \times 1''.6$  at the focal plane. It is designed to have a wide field view of  $28' \times 28'$ . The primary motivation of the *MiSuME* project is a multi-band photometry of  $\gamma$ -ray bursts (GRBs) and their afterglows at very early phases, but the telescopes are also actively used for multi-color optical monitoring of more than 30 blazars and other interesting Galactic or extragalactic sources. These telescopes are automatically operated and respond to GRB alerts and transient events like active galactic nucleus (AGN) flares.

*MiSuME* observed 3C 454.3 almost every day from 2007 November 22 to December 6 so as to provide simultaneous data with *AGILE* and *Suzaku*. All raw  $g'$ ,  $R_c$ , and  $I_c$  frames were corrected for the dark, bias and flat field by using IRAF version 2.12 software. Instrumental magnitudes were obtained via aperture photometry using DAOPHOT (Stetson 1987) and SExtractor (Bertin & Arnouts 1996). Calibration of the optical source magnitude was conducted by differential photometry with respect to the comparison stars sequence reported by Raiteri et al. (1998) and González-Pérez et al. (2001). The fluxes are corrected for the Galactic extinction corresponding to a reddening of  $E(B - V) = 0.108$  mag (Schlegel et al. 1998). The  $R_c$ -optical light curve between

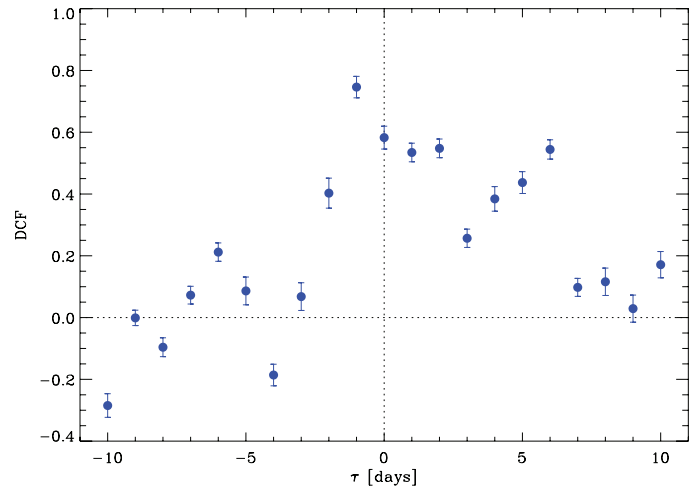


**Figure 6.** 3C 454.3 DCF between the  $\gamma$ -ray and optical ( $R$ -band) magnitudes. (A color version of this figure is available in the online journal.)

November 30 and December 6 is shown in Figure 1 (bottom panel, green circles).

## 7. MID-INFRARED OBSERVATIONS

Given the high  $\gamma$ -ray activity detected by *AGILE* from 3C 454.3, we also requested and obtained a DDT for a mid-infrared follow-up by *Spitzer* (Werner et al. 2004). The DDT was approved for two epochs for a total duration of 0.8 hr of the Infrared spectrograph (IRS; Houck et al. 2004) providing short-low and long-low observations of 3C 454.3 scheduled for December 13 (starting at MJD 54447.410) and 15 (starting at MJD 54449.403). Both observations provided us with a low-resolution spectrum ( $\Delta\lambda/\lambda \sim 80$ ) in the energy range  $\sim 5\text{--}38 \mu\text{m}$ . Data were acquired in the IRS standard staring mode: observations were obtained at two positions along the slit to enable sky subtraction. Each ramp duration was set to 14.68 s with a number of cycles equal to 5. Each set of data was processed with the IRS Standard Pipeline *SMART* developed at the *Spitzer* Science Center to produce calibrated data frames (Basic Calibrated Data, BCD, files). Moreover, the BCD files covering the same spectral range were coadded and then sky-subtracted spectra were obtained. The absolute flux calibration was estimated by using the electron-to-Jy conversion polynomial given in the appropriate *Spitzer* calibration file. In Figure 5, we present the two spectra obtained on December 13 and 15. We performed a linear fit of the two, obtaining fluxes equal to  $(1.59 \pm 0.02) \times 10^{-10}$  and  $(1.38 \pm 0.02) \times 10^{-10} \text{ erg cm}^{-2} \text{ s}^{-1}$  for December 13 and 15, respectively.

## 8. DISCUSSION

### 8.1. Timing Analysis

We investigated the emission of the blazar 3C 454.3 during a multifrequency campaign performed in the first half of 2007 December. The source was found to be in flaring state with an average  $\gamma$ -ray flux above 100 MeV of  $\sim 250 \times 10^{-8} \text{ photons cm}^{-2} \text{ s}^{-1}$ , which is typical of its high  $\gamma$ -ray state (Vercellone et al. 2008, 2009; Anderhub et al. 2009). As in the case of the previous multifrequency campaign (2007 November; Vercellone et al. 2009), the source was continuously monitored in  $\gamma$ -rays as well as in the optical energy bands. In both energy bands, the source exhibited comparable flux variations of the

order of  $\sim 4$ : this argues for an EC model. Moreover, we deeply studied the optical- $\gamma$ -ray correlation by means of a discrete correlation function (DCF; Edelson & Krolik 1988; Hufnagel & Bregman 1992) applied to the optical and  $\gamma$ -ray light curves reported in Figure 1. This analysis revealed  $\lesssim$ one-day delay of the  $\gamma$ -ray emission with respect to the optical one (see Figure 6). Indeed, the DCF maximum at a time lag of  $\tau = -1$  day corresponds to a centroid of  $\tau = -0.56$  days, whose uncertainty can be estimated by means of the Monte Carlo method known as “flux redistribution/random subset selection” (Peterson et al. 1998; Raiteri et al. 2003). By running 1000 simulations we found  $\tau = -0.6^{+0.7}_{-0.5}$  day at  $1\sigma$  confidence level. We also performed the DCF reducing the data binning down to 12 hr between December 5 and 16, keeping the one-day binned  $\gamma$ -ray light curve for the data before December 5 (MJD = 54,439.524). This shows a peak at  $-1$  day with centroid at  $-0.54$  days which is in agreement with the result obtained with the one-day binned  $\gamma$ -ray light curve. In this case, the Monte Carlo method is not able to provide a reliable estimate of the error on the time lag due to the larger uncertainties on the  $\gamma$ -ray fluxes.

The evidence of this time lag again suggests the dominance of the EC model: such a delay is compatible with the typical blob dimensions and the corresponding crossing time of the external seed photons (Sokolov et al. 2004). We note that this evidence agrees with what was found by Bonning et al. (2009).

Particularly interesting is the source optical flare recorded by WEBT on December 12 (Raiteri et al. 2008a). The source experienced an exceptional variability in less than 3 hr. Raiteri et al. (2008a) interpreted this event as a variation in the properties of the jet emission. This unusual event clearly required an intraday analysis of the  $\gamma$ -ray data. This analysis depends on the source brightness and the instrumental sensitivity. Given the  $\gamma$ -ray flux level of 3C 454.3 reached between 2007 December 5 and 2007 December 16, we obtained a data binning not smaller than 12 hr (Figure 7, top panel). This analysis showed an enhancement of more than a factor of 2 of the  $\gamma$ -ray flux during the second half of 2007 December 12, that remarkably includes the time of the optical event (see vertical lines in Figure 7). The enhancement by a factor of  $\sim 2$  of the  $\gamma$ -ray flux was comparable with the 1.1 mag optical brightening. This could support the evidence of a change in the jet emission in the EC scenario. The 12 hr  $\gamma$ -ray light curve could constrain a possible delay between the  $\gamma$ -ray emission and the optical one within 12 hr, shorter than ever observed before for this source.

### 8.2. Spectral Modeling

As described in the previous section, the 2007 December multifrequency campaign was characterized by ToO carried out in mid-infrared (*Spitzer*), soft X-ray (*Suzaku*, *Swift*), hard X-ray (*Suzaku*) and radio-to-optical, and  $\gamma$ -ray monitoring. These observations allowed us to obtain the SED of this blazar with a wide multifrequency coverage for three different epochs: December 5, 13, and 15. At these dates, the SED in X-rays shows a softening toward lower frequencies that can be due to two causes: (1) a contribution from bulk Comptonization by cold electrons in the jet (Celotti et al. 2007) and (2) the emergence of the SSC contribution in soft X-rays from the more energetic EC component due to the disk and the BLR. The mid-infrared *Spitzer* data and optical data available in December 13 and 15 (which well define the synchrotron peak), combined with the resolved X-ray spectrum and the  $\gamma$ -ray data, constrain the model parameters, arguing for the latter case; the SSC emergence is a natural and inevitable consequence of the simultaneous mod-

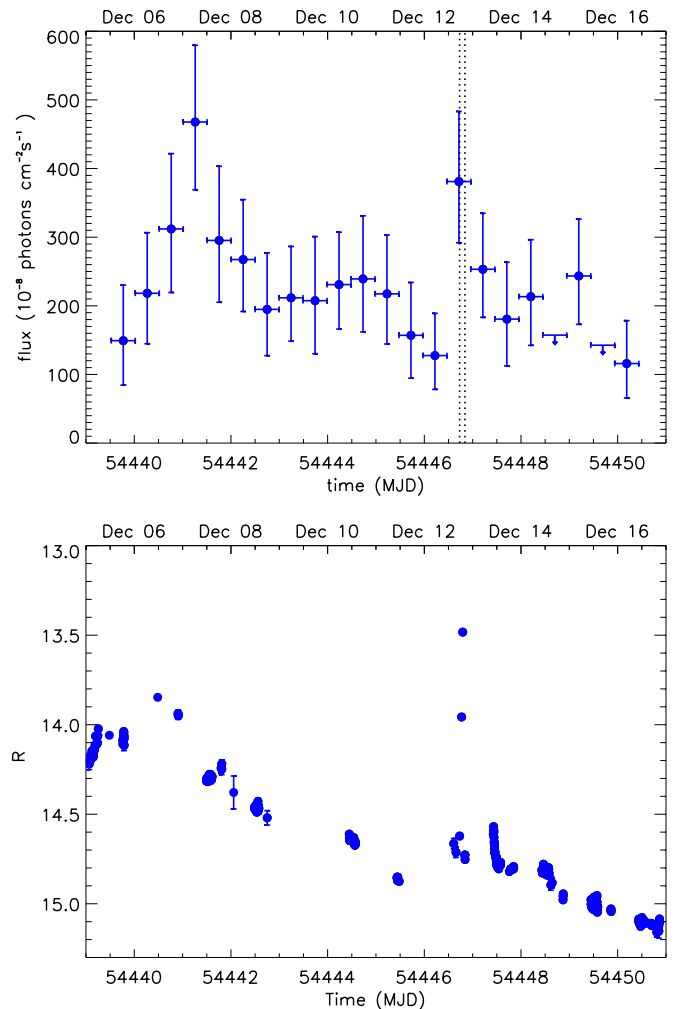


**Figure 7.** Top panel:  $\gamma$ -ray 12 hr light curve above 100 MeV during the period between 2007 December 5 and 2007 December 16 when the source was at  $30^\circ$  in the *AGILE* FoV. The vertical lines mark the time ( $<3$  hr) of the exceptional optical event of 2007 December 12; bottom panel:  $R$ -band optical light curve obtained during the period reported above.

(A color version of this figure is available in the online journal.)

eling of the broadband SED. Nevertheless, some contribution from bulk Comptonization cannot be ruled out.

We first considered the state of December 13 and 15 in which we have simultaneous radio, mid-infrared, optical, X-ray, and  $\gamma$ -ray data. In these epochs, 3C 454.3 was in a different state with respect to the one analyzed in November: optical and UV fluxes appeared lower by a factor of 2–3, suggesting the synchrotron bump peaking at a frequency 5–10 times lower than the one observed in November, as confirmed also from the mid-infrared data. On the other hand, the soft X-ray data were only a little bit lower than in November. Despite the softer synchrotron bump,  $\gamma$ -ray data showed in the SED the persistence of a hard peak at  $\simeq 1$  GeV, similar to the higher states observed by *AGILE* in 2007 July and 2007 November (Anderhub et al. 2009; Vercellone et al. 2009). In fact, the December  $\gamma$ -ray spectrum (characterized by a photon index of  $\sim 1.78$ ) is consistent with those obtained during the two previous *AGILE* observations.

We attempted to fit the SEDs with a one-zone SSC model, adding the contribution of external seed photons coming from an accretion disk and a BLR (Raiteri et al. 2007). With this model, we succeeded in fitting the synchrotron peak as well as the X-ray data assuming parameters similar to the November

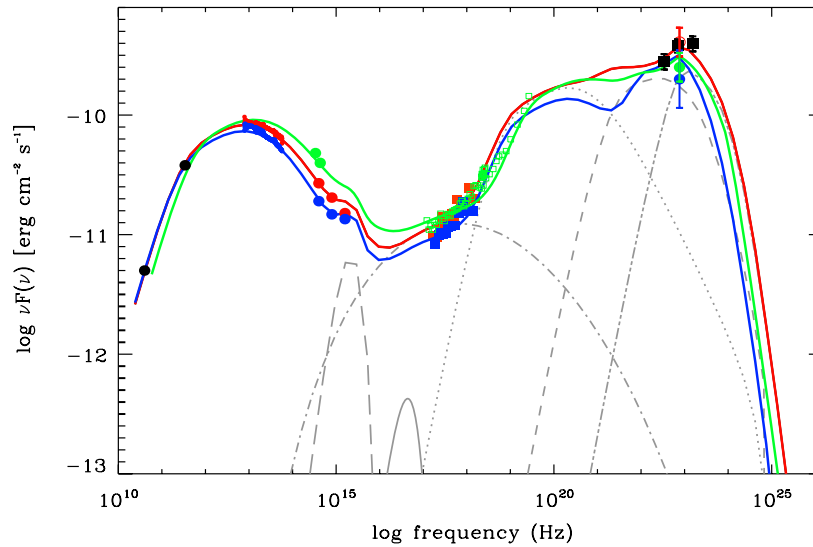


**Figure 8.** 3C 454.3 SEDs for 2007 December 5, 13, and 15 (green, red, and blue solid lines, respectively). The  $\gamma$ -ray spectrum for  $E > 100$  MeV (black squares), extracted from data acquired between December 5 and 16, and the radio points (black circles) from Raiteri et al. (2008a) are also reported. The gray lines represent the contribution of the disk (long dashes), corona (solid), SSC (dot-dashed), EC disk (dotted), EC BLR (dashed), and EC corona (dash dot dot) to the December 13 model.

**Table 2**  
Model Parameters for the December States of 3C 454.3

Observation Date	$\Gamma$	$B$ (gauss)	$R$ (cm)	$K$ ( $\text{cm}^{-3}$ )	$\gamma_b$	$\gamma_{\min}$	$a_l$	$a_h$
2007 Dec 5	18	2.5	$2.2 \times 10^{16}$	50	$3 \times 10^2$	30	2.3	4.2
2007 Dec 13	18	2	$2.2 \times 10^{16}$	52	$3.5 \times 10^2$	38	2.3	4.2
2007 Dec 15	18	2	$2.2 \times 10^{16}$	52	$3.2 \times 10^2$	35	2.3	4.2

ones, but a lower  $\gamma_b \simeq 350$  was required to account for the softness of the synchrotron bump: with this  $\gamma_b$  the EC from a standard BLR peaks at  $h\nu \simeq h\nu_{\text{soft}} \Gamma \gamma_b^2 \delta / (1+z) \sim 10^8$  eV. This is in contrast to the observed hardness of the  $\gamma$ -ray spectrum up to 1 GeV ( $h\nu_{\text{soft}} \simeq 10$  eV is the typical energy of the external source as seen by the observer). We note that the EC by the disk can account for the rising hard X-ray portion of the SED, which did not show clear variability. Nevertheless, we note that both the disk and BLR components cannot account for the hardness of the  $\gamma$ -ray spectrum. Thus, we consider a further external source of seed photons.

A possible candidate for this source is the hot extended corona that must be consistently produced in steady accretion/ejection flows as shown by MHD numerical simulations (Tzeferacos et al. 2009). Hence, we considered a one-zone SSC model plus the contribution by external seed photons coming from the accretion disk, the BLR, and the hot corona. We adopted a spherical blob with radius  $R = 2.2 \times 10^{16}$  cm and a broken power law for the electron energy density in the blob:

$$n_e(\gamma) = \frac{K \gamma_b^{-1}}{(\gamma/\gamma_b)^{a_l} + (\gamma/\gamma_b)^{a_h}}, \quad (1)$$

where  $\gamma$  is the electron Lorentz factor assumed to vary between  $10 < \gamma < 10^4$ , while  $a_l = 2.3$  and  $a_h = 4.2$  are the pre- and post-break electron distribution spectral indices, respectively. We assumed that the blob contained a random magnetic field  $B = 2$  gauss and that it moved with the bulk Lorentz Factor  $\Gamma = 18$  at an angle  $\Theta_0 = 1^\circ$  ( $\delta \simeq 33$ ) with respect to the line of sight. The density parameter into the blob is  $K = 52 \text{ cm}^{-3}$ .

The bolometric luminosity of the accretion disk is  $L_d = 3 \times 10^{46} \text{ erg s}^{-1}$ , and it is assumed to lie at 0.01 pc from the blob; we assumed a BLR distance of 1.5 pc, reprocessing a 10% of the irradiating continuum. We assumed for the disk a blackbody

spectrum peaking in UV (see Tavecchio & Ghisellini 2008; Raiteri et al. 2008b). Finally, we added the hot corona photons surrounding the jet as a blackbody spectrum of  $T = 10^6$  K and  $L_h = 10^{45} \text{ erg s}^{-1}$ , and a distance of 0.5 pc from the blob. The SEDs of both December 13 and 15 could be fitted with almost the same parameters (see red and blue solid lines in Figure 8). The high-energy portion of the electron density becomes softer on December 15 as the same electrons should be accelerated with less efficiency than on December 13.

Remarkably, the lower  $\gamma_b$  required in the epochs considered here makes the BLR a too soft contributor at GeV energies, while the contribution of the hot corona succeeded to account for the persistence of the hard  $\gamma$ -ray spectra measured by *AGILE*.

On December 5, the low-energy peak of the SED is less constrained with respect to the December 13 and 15 ones due to the lack of the mid-infrared data. On the other hand, the *Suzaku* X-ray data (green points in Figure 8) better constrain the rise of the IC emission. We fitted this SED with almost the same model assumed for the other two epochs, but the higher optical flux and the lower  $\gamma$ -ray flux detected with respect to December 13 required a higher magnetic field and a lower  $\gamma_b$  (see Table 2).

Given the different  $\gamma$ -ray state of the source analyzed in the November and December campaigns, we compared the particle injection luminosity,  $L_{\text{inj}}$ , measured during the two multiwavelength campaigns. This is expressed by means of the following formula:

$$L_{\text{inj}} = \pi R^2 \Gamma^2 c \int [d\gamma m_e c^2 \gamma n(\gamma)]. \quad (2)$$

We found the particle injection luminosity of December to be  $6 \times 10^{43} \text{ erg s}^{-1}$ , a factor of 5 lower than the November one. This difference is due to both the lower  $\gamma_b$  and  $\gamma_{\min}$  values needed to reproduce the SED in the states of December.



## 9. CONCLUSIONS

We reported in this paper the main results of a multifrequency campaign on the blazar 3C 454.3 performed in 2007 December. The source was simultaneously observed in mid-infrared, optical, X-ray, and  $\gamma$ -ray energy bands, which provided us with a wide data set aimed at studying the correlation between the emission properties at lower and higher frequencies. We summarize below the major results.

1. The  $\gamma$ -ray emission from 3C 454.3 shows variations on a daily timescale.
2. The simultaneous monitoring of the source in the optical and  $\gamma$ -ray energy bands allowed us to determine a possible  $\lesssim$ one-day delay of the  $\gamma$ -ray emission with respect to the optical one.
3. The extraordinary optical activity (lasting less than 3 hr), observed on December 12, has a counterpart in the  $\gamma$ -ray data. A possible delay between the  $\gamma$ -ray emission and the optical one is constrained within 12 hr.
4. We found that a leptonic model with an EC on seed photons from the disk and BLR does not succeed in accounting for both the “hardness” of the  $\gamma$ -ray spectrum and the “softness” of the synchrotron emission, and requires an additional component. We argued that a possible candidate for it is the hot corona ( $T \sim 10^6$  K) surrounding the disk.

*AGILE* is a mission of the Italian Space Agency, with participation of the Istituto Nazionale di Astrofisica (INAF) and the Istituto Nazionale di Fisica Nucleare (INFN). This work was partially supported by ASI grants I/R/045/04, I/089/06/0, I/011/07/0, and by the Italian Ministry of University and Research (PRIN 2005025417). INAF personnel at ASDC are under ASI contract I/024/05/1. This work is partly based on data taken and assembled by the WEBT collaboration and stored in the WEBT archive at the Osservatorio Astronomico di Torino-INAF (<http://www.oato.inaf.it/blazars/webt/>). This work is based in part on observations made with the *Spitzer Space Telescope*, which is operated by the Jet Propulsion Laboratory, California Institute of Technology under a contract with NASA. The IRS was a collaborative venture between Cornell University and Ball Aerospace Corporation funded by NASA through the Jet Propulsion Laboratory and Ames Research Center. SMART was developed by the IRS Team at Cornell University and is available through the Spitzer Science Center at Caltech.

## REFERENCES

- Abdo, A. A. (Fermi/LAT Collaboration) 2009, *ApJ*, 699, 817  
 Anderhub, H., et al. 2009, *A&A*, 498, 83

- Barthelmy, S. D., et al. 2005, *Space Sci. Rev.*, 120, 143  
 Bertin, E., & Arnouts, S. 1996, *A&AS*, 117, 393  
 Bonning, E. W., et al. 2009, *ApJ*, 697, L81  
 Burrows, D. N., et al. 2005, *Space Sci. Rev.*, 120, 165  
 Celotti, A., Ghisellini, G., & Fabian, A. C. 2007, *MNRAS*, 375, 417  
 Conconi, P., et al. 2004, *Proc. SPIE*, 5492, 1602  
 Edelson, R. A., & Krolik, J. H. 1988, *ApJ*, 333, 646  
 Feroci, M., et al. 2007, *Nucl. Instrum. Methods Phys. Res. A.*, 581, 728  
 Gehrels, N., et al. 2004, *ApJ*, 611, 1005  
 Ghisellini, G., Celotti, A., Fossati, G., Maraschi, L., & Comastri, A. 1998, *MNRAS*, 301, 451  
 Ghisellini, G., Foschini, L., Tavecchio, F., & Pian, E. 2007, *MNRAS*, 382, L82  
 Giommi, P., et al. 2006, *A&A*, 456, 911  
 González-Pérez, J. N., Kidger, M. R., & Martín-Luis, F. 2001, *AJ*, 122, 2055  
 Hill, J. E., et al. 2004, *Proc. SPIE*, 5165, 217  
 Houck, J. R., et al. 2004, *ApJS*, 154, 18  
 Hufnagel, B. R., & Bregman, J. N. 1992, *ApJ*, 386, 473  
 Katarzyński, K., & Ghisellini, G. 2007, *A&A*, 463, 529  
 Kokubun, M., et al. 2007, *PASJ*, 59, 53  
 Koyama, K., et al. 2007, *PASJ*, 59, 23  
 Labanti, C., et al. 2009, *Nucl. Instrum. Methods Phys. Res. A*, 598, 470  
 Mattox, J. R., et al. 1996, *ApJ*, 461, 396  
 Mitsuda, K., et al. 2007, *PASJ*, 59, 1  
 Perotti, F., Fiorini, M., Incorvaia, S., Mattaini, E., & Sant’Ambrogio, E. 2006, *Nucl. Instrum. Methods Phys. Res. A*, 556, 228  
 Peterson, B. M., Wanders, I., Horne, K., Collier, S., Alexander, T., Kaspi, S., & Maoz, D. 1998, *PASP*, 110, 660  
 Pian, E., et al. 2006, *A&A*, 449, L21  
 Prest, M., Barbiellini, G., Bordignon, G., Fedel, G., Liello, F., Longo, F., Pontoni, C., & Vallazza, E. 2003, *Nucl. Instrum. Methods Phys. Res. A*, 501, 280  
 Raiteri, C. M., Villata, M., Lanteri, L., Cavallone, M., & Sobrito, G. 1998, *A&AS*, 130, 495  
 Raiteri, C. M., et al. 2003, *A&A*, 402, 151  
 Raiteri, C. M., et al. 2007, *A&A*, 473, 819  
 Raiteri, C. M., et al. 2008a, *A&A*, 491, 755  
 Raiteri, C. M., et al. 2008b, *A&A*, 485, L17  
 Roming, P. W. A., et al. 2005, *Space Sci. Rev.*, 120, 95  
 Schlegel, D. J., Finkbeiner, D. P., & Davis, M. 1998, *ApJ*, 500, 525  
 Serlemitsos, P. J., et al. 2007, *PASJ*, 59, 9  
 Sikora, M., Moderski, R., & Madejski, G. M. 2008, *ApJ*, 675, 71  
 Sokolov, A., Marscher, A. P., & McHardy, I. M. 2004, *ApJ*, 613, 725  
 Stetson, P. B. 1987, *PASP*, 99, 191  
 Takahashi, T., et al. 2007, *PASJ*, 59, 35  
 Tavani, M., et al. 2008, *Nucl. Instrum. Methods Phys. Res. A*, 588, 52  
 Tavani, M., et al. 2009, *A&A*, 502, 995  
 Tavecchio, F., & Ghisellini, G. 2008, *MNRAS*, 386, 945  
 Tavecchio, F., et al. 2002, *ApJ*, 575, 137  
 Tosti, G., Chiang, J., Lott, B., Do Couto E Silva, E., Grove, J. E., & Thayer, J. G. 2008, *ATel*, 1628, 1  
 Tosti, G., et al. 2004, *Proc. SPIE*, 5492, 689  
 Tzeferacos, P., Ferrari, A., Mignone, A., Bodo, G., & Massaglia, S. P. 2009, *MNRAS*, 400, 820  
 Vercellone, S., et al. 2008, *ApJ*, 676, L13  
 Vercellone, S., et al. 2009, *ApJ*, 690, 1018  
 Villata, M., et al. 2006, *A&A*, 453, 817  
 Villata, M., et al. 2007, *A&A*, 464, L5  
 Werner, M. W., et al. 2004, *ApJS*, 154, 1  
 Zerbi, F. M., et al. 2004, *Proc. SPIE*, 5492, 1590